OECD/NEA−VATTENFALL T-JUNCTION BENCHMARK SPECIFICATIONS
(FINAL VERSION, JULY 2009)

A1. GEOMETRICAL DATA

The complete test rig, which is located at the Vattenfall Research and Development Laboratory at Älvkarleby, Sweden, is illustrated in Fig. A1. Cold water is supplied from a high-level reservoir designed to maintain a constant water level independent of the flow rate. A stagnation chamber of diameter 400 mm is mounted at the beginning of the horizontal pipe, and contains two perforated plates, a tube bundle (inner diameter of the tubes is 10 mm and the length 150 mm), a third perforated plate and finally a contraction with an area ratio of about 8:1. The stagnation chamber is designed to provide a high quality flow without large-scale turbulence or secondary flows. The stagnation chamber is connected to a 10 m long pipe section made from ABS plastic, which is followed by a Plexiglas section extending 1270 mm upstream of the T-junction. The total upstream length of the pipe, with constant diameter D_2=140 mm, is thus more than 80 pipe diameters. The flow rate is measured using an electro-magnetic flow meter (labelled Q2 in Fig. A1).

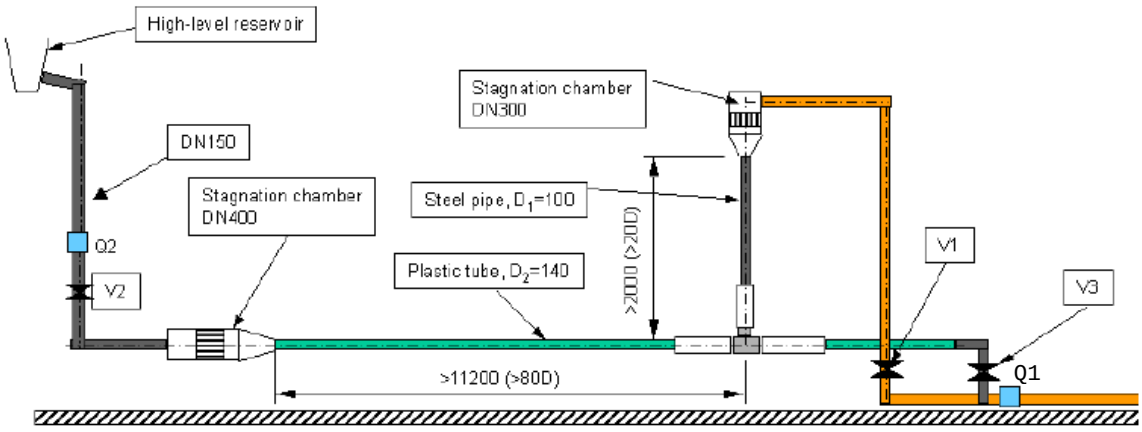

Figure A1: Schematic of Vattenfall T-junction test rig

The hot water is taken from a 70 m^3 reservoir, and a pump is used to feed the model. The rotational speed of pump is automatically controlled to maintain a constant flow rate through flow meter Q1. A stagnation chamber (diameter 300 mm), similar to that on the cold water side, is used here too, though with the water feed being supplied from the side by means of a flow distributor. The stagnation chamber is connected to a steel pipe of inner diameter 100 mm, which gives an area contraction ratio of 9. The total distance with constant diameter (D_1=100 mm) upstream of the T-junction is approximately 20 pipe diameters for the hot water pipe. Fully developed pipe flow cannot be obtained in this case, though the flow quality is expected to be good due to presence of the stagnation chamber.

A close-up of the test section is given in Fig. A2. The actual tee is made from a solid Plexiglas block through which circular channels have been drilled into which the hot and cold water feed pipes fit, as illustrated in Fig. A3.

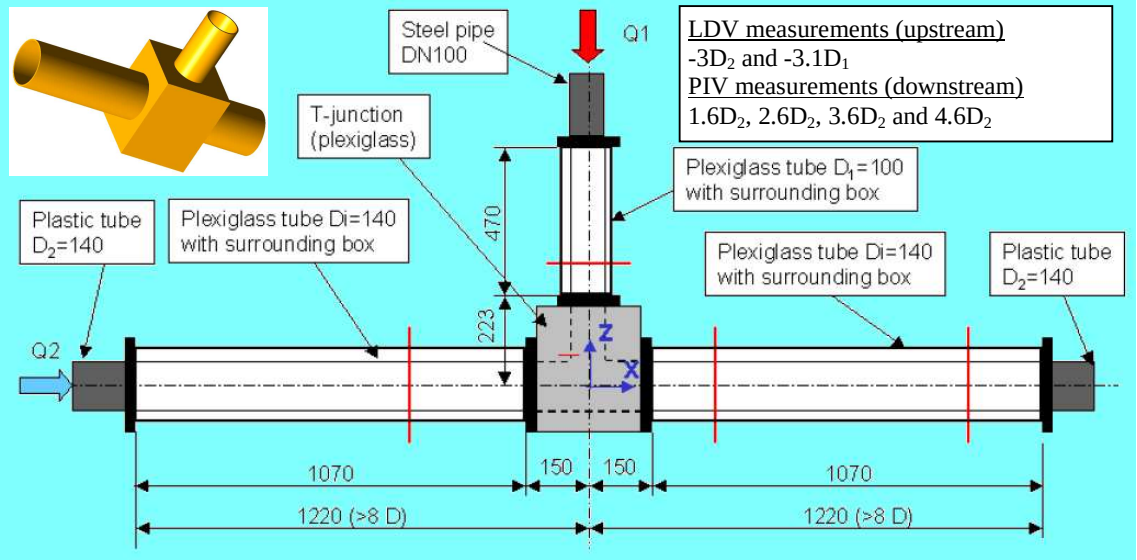

Figure A2: Schematic of T-junction with Plexiglas sections

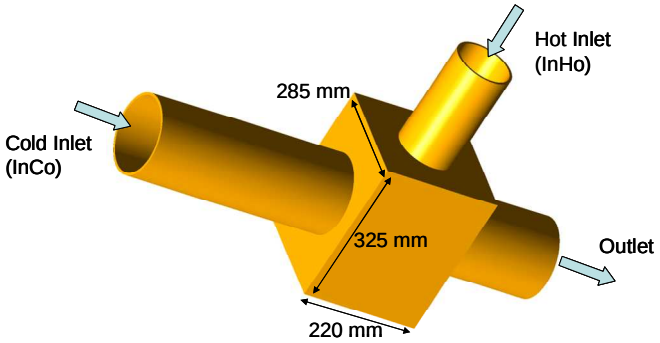

Figure A3: Schematic of the T-junction block showing dimensions

The circular channels within the block are of the same diameter as the attached pipes and are considered hydraulically smooth, though no specific measurement of the roughness has been performed. The tee has been machined with internal "sharp" edges: i.e. the edge at the intersection between the main and branch channels within the block has been only slightly ground. The exact radius of curvature has not been measured, but is certainly smaller than 0.2 mm. Overall dimensions also appear in Table A1.

Table A1: Dimensions of T-junction test section

Component	**Material**	**Dimensions (mm)**
Main inlet pipe	Plexiglas	Length: 1070; ID: 140; OD: 150
Branch inlet pipe	Plexiglas	Length: 470; ID: 100; OD: 110
Outlet pipe	Plexiglas	Length: 1070; ID: 140; OD: 150
Tee Block	Plexiglas	Length (x): 220; Width (y): 285, Height (z): 325 Main channel diameter: 140 Branch channel diameter: 100

For the cold (horizontal) inlet pipe, LDA measurements have been taken 3 diameters upstream of the junction. These confirm the fully developed flow conditions expected from

the length of the feed line (see Section A3.1). Similar LDA measurements have been taken 3.1 diameters upstream of the junction for the hot inlet. Here, the flow is not fully developed (see Section A3.2).

Close to the T-junction, each of the three pipes (two inlet and one outlet) is surrounded by a rectangular water box; see Fig. A2. This is necessary to avoid distortions of the laser beams at the curved surfaces of the pipes when velocity measurements are made. For the present benchmark experiment, no new upstream velocity measurements have been carried out, since it was considered those taken during the previous test series in 2006 were adequate (see explanation given in Section A3). Downstream, the box was only filled with water – at ambient (15^{o}C) temperature – when velocity measurements (using PIV) were being made, these measurements being carried out under cold operating conditions (i.e. cold water supply to both inlets).

At the time the thermocouple measurements were taken, the box was emptied of water, and contained air at ambient (15^{o}C) temperature. Consequently, heat losses through pipe walls are generally considered negligible. The hot inlet pipe above the test section is made of steel (labelled in Fig. A1), and the pipe is not insulated. However, temperatures taken in the stagnation chamber and just upstream of the junction show differences of 0.1-0.2oC, within the tolerances of the thermocouple measurements. Hence it can be assumed there are no measurable heat losses through the exposed heat pipe. Nonetheless, exact dimensions and material properties of the inlet pipes and water boxes can be supplied by the organizers to specific participants who wish to model them explicitly.

A2. MATERIAL PROPERTIES

The working fluid in this test is deionized tap water between 19°C and 36°C. It is considered that the physical properties are adequately described by the ASME steam tables (1967), with additional information on the thermal expansion coefficient from the book of Incropera and DeWitt (1990). Values are displayed in Table A2 for temperatures of relevance. Note that these data are supplied as a guide only.

Table A2: Physical properties of water

Temperature (°C)	**Density (kg/m^3)**	**Thermal conductivity (W/m K)**	**Dynamic viscosity (N s/m^2)**	**Heat capacity (J/kg K)**	**Molecular Prandtl number (-)**
15	999.2	0.5911	1.138E-3	4186	8.058
20	998.3	0.5996	1.002E-3	4182	6.988
25	997.2	0.6076	0.8904E-3	4179	6.125
30	995.8	0.6151	0.7977E-3	4178	5.419
35	994.1	0.6221	0.7196E-3	4178	4.833
40	992.3	0.6287	0.6533E-3	4178	4.342

Temperature (K)	**Coefficient of volumetric expansion (K^{-1})**
285	114.1E-6
290	174.0E-6
295	227.5E-6
300	276.1E-6
305	320.6E-6
310	361.9E-6
315	400.4E-6

The Plexiglas is of low conductivity, and the temperatures are at or close to ambient everywhere (≈15°C), so it is not anticipated that heat losses from the water in the test section will be important (see remarks above). However, the material properties of the Plexiglas material are as listed in Table A3 for reference, the values being based on the specifications delivered by the supplier.

Table A3: Physical properties of Plexiglas

Density (kg/m^3)	**Thermal conductivity (W/m K)**	**Heat capacity (J/kg K)**	**Coefficient of volumetric expansion (K^{-1})**
1200.0	0.190	1460	240.0E-6

A3. INLET BOUNDARY CONDITIONS

The volumetric flow rates used in the test are given in Table A4, together with the locations where the velocity distributions over the pipe cross-sections were measured (the left and upper red lines in Fig. A2). The temperatures for the cold and hot inlets are also given at these cross-sections. As a consequence of the thorough flow mixing in the upstream stagnation chambers, the temperatures of the inflowing streams were assumed to be uniform at the measuring locations, and only one thermocouple was placed there. The reading taken is that given in the 2nd column of Table A4.

Table A4: Inlet temperatures and flow rates

Inlet/designation	**Temperature (^{o}C)**	**Pipe diameter (mm)**	**Measuring location (mm)#**	**Volumetric flow rate (litres/s)**
Main/InCo	19	140 (D_2)	-420 (-3D_2)	9.0
Branch/InHo	36	100 (D_1)	-310 (-3.1D_1)	6.0

The negative sign indicates upstream of the junction mid-point (i.e. the point where the centrelines of the pipes cross)

The inlet velocity profiles presented in this section are taken from an earlier test (Westin et. al, 2008) in which the volumetric flow ratio between the main and branch streams was 2. In the present test (flow ratio 1.5), the flowrate in the hot inlet was kept the same as before (6 l/s), whereas the one in the cold inlet was 9.0 l/s instead of 12.0 l/s used previously. Since the velocity profile is fully developed in the cold inlet, the results presented below can simply be scaled to fit the present flowrate.

In the earlier test, the velocity measurements were taken at upstream locations using a two-component LDA system, which gave one component of velocity in the main flow direction (i.e. parallel to the axis of the pipe) and one component transverse to this. The coordinate systems adopted in the measuring planes of the two upstream pipes are shown in Fig. A4.

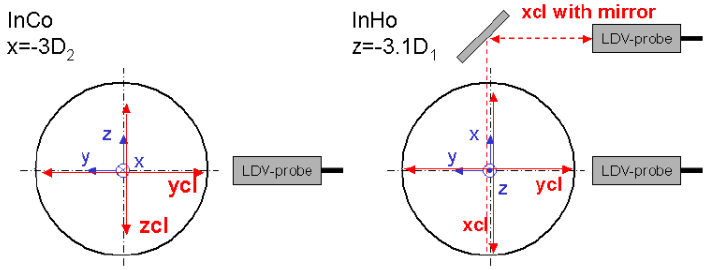

Figure A4: Overview of the upstream LDV measurement orientations

Velocity profiles and turbulence statistics are available in the two perpendicular directions defined in Fig. A4 for the main (InCo) and branch (InHo) pipes, respectively. It should be noted that special means to obtain accurate near-wall measurements have not been undertaken. This should be kept in mind when measurement data close to the pipe walls are used, since the accuracy of these data can be expected to be lower than for those away from the wall.

A3.1 Main Pipe: InCo

The measuring plane is -3D_2 upstream of the centre of the T-junction. Profiles are drawn in the left column of Fig. A5. Note that the streamwise mean velocity component (U) is scaled with the bulk velocity; U_{bulk}, while the other velocity components are scaled with the mean centreline velocity, U_{cl}, where U_{cl} = 1.17 U_{bulk}. The two cross-stream profiles zcl and ycl for the streamwise component are in good agreement, which is to be expected given that the flow should be axisymmetric. The higher moments, skewness and flatness, also show typical values for fully-developed turbulent flow. The definitions of these quantities are listed here:

Mean $U = \bar{u} = \frac{1}{n}\sum_{i=1}^{n} u_i$ RMS $U_{rms} = \left(\overline{(u-\bar{u})^2}\right)^{1/2}$

Skewness $S = \left(\overline{(u-\bar{u})^3}\right)/U_{rms}^3$ Flatness $F = \left(\overline{(u-\bar{u})^4}\right)/U_{rms}^4$

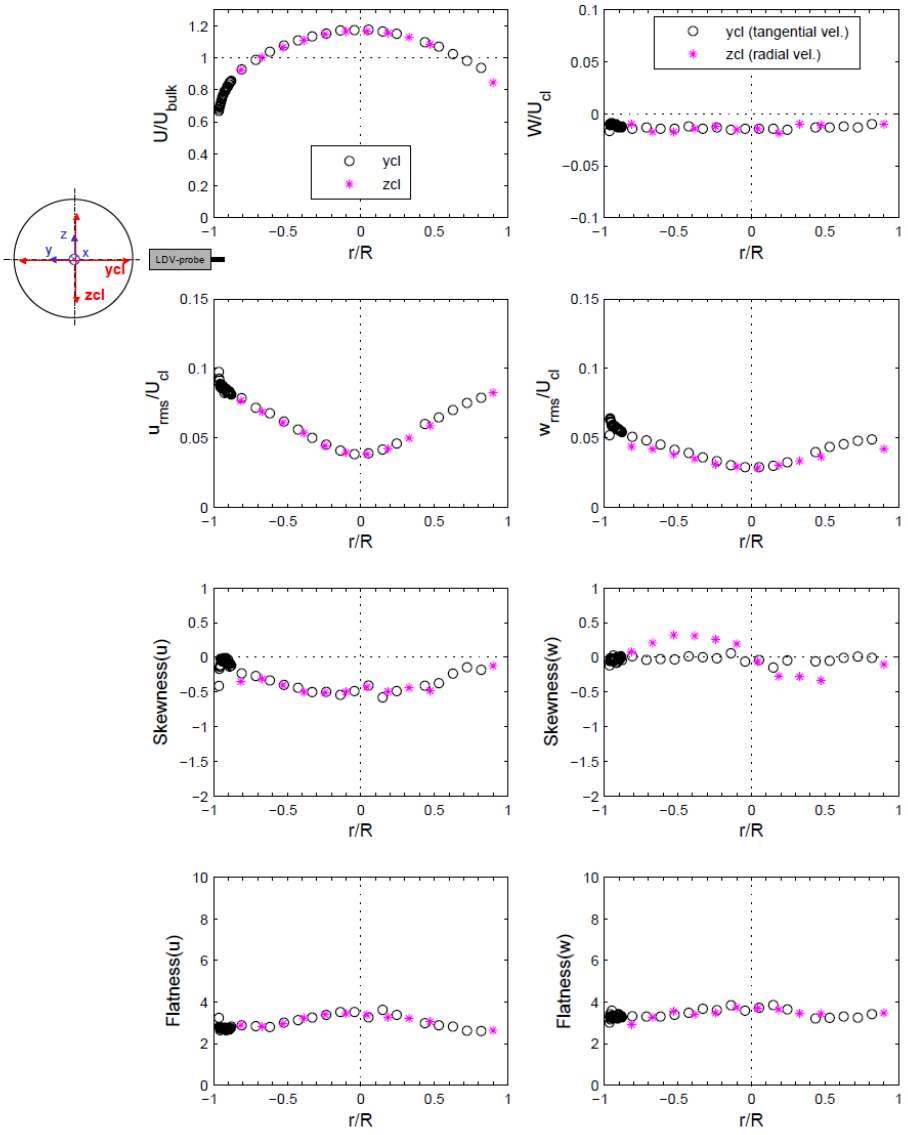

Figure A5: Velocity measurements in the cold inlet pipe at x = -3D_2, measured along zcl and ycl. The left column shows data for the axial velocity component (u), and the right column shows corresponding data for the transverse components.

The plots in the right column of Fig. A5 refer to the transverse velocity components. Note that these are scaled with respect to the mean centreline velocity U_{cl} and not the bulk velocity. For convenience, all these data have been reproduced in tabular form at the end of this document.

The Reynolds shear stresses are given in Fig. A6. The correlation between the streamwise and the tangential (azimuthal) velocity component (profile ycl) should be zero for pure axisymmetric flow, and the values in the Figure are close to zero, except for some scatter near the wall. The correlation between the radial and the streamwise velocity fluctuations (profile zcl) is more interesting. For fully turbulent pipe flow, the Reynolds stress can be exactly derived (e.g. Tennekes and Lumley, 1972), and takes the following form:

$$\overline{uw} = u_\tau^2\left(\frac{r}{R} + \upsilon\frac{\partial U}{\partial r}\right)$$

$$u_\tau = \text{friction velocity} = \sqrt{\tau_w / \rho}$$

The second term within the brackets is small, except close to the pipe wall, so the uw-profile should be linear in the central part of the pipe. A linear fit has been applied to the data in Fig. A6, and the friction velocity (u_τ), scaled with respect to the centreline velocity U_{cl}, derived accordingly. The inverse gives the ratio $U_{cl}/u_\tau = U_{cl}^+ = 25.8$. The ratio is dependent on Reynolds number. Zagarola and Smits (1998) report $U_{cl}^+ \approx 25.5$ for Re = 98 000, very close the values found here.

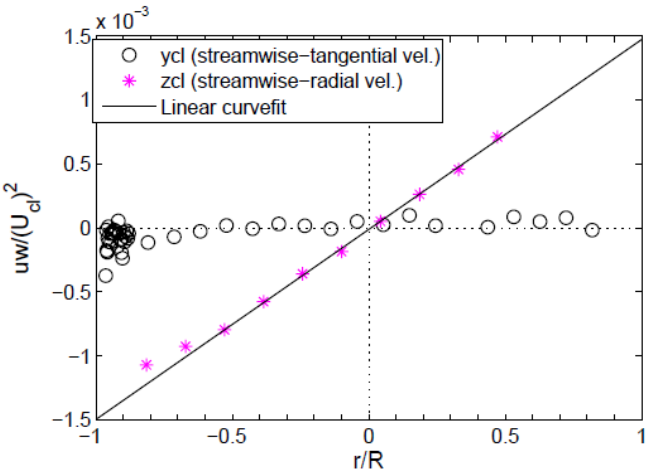

Figure A6: Reynolds shear stress (uw) in the cold inlet pipe at x = -3D_2. The straight line is a fit to the central part of the data (-0.5 < r/R < 0.5).

Figure A7 shows the measured streamwise mean velocity, plotted in wall coordinates, using a logarithmic scale for the distance from the wall. Note that $y^+ = 0$ corresponds to the inner pipe wall in this plot. The friction velocity obtained from the Reynolds stress profile in Fig. A6 has been used (u_τ = 0.026 m/s), which gives a viscous length scale $l^* = \mu/\rho u_\tau \approx 40$ µm. However, the slope of the log-region is very sensitive to the estimated wall position, which results in an uncertainty. In Fig. A7, the velocity profile is plotted according to the original coordinates obtained from the measurements, but also with the coordinates shifted by –0.7 mm in the y-direction. It should also be noted that with a length scale of the order of 40 µm the measurement volume and the spatial resolution for the LDV measurements is around Δy^+ = 30, which means that the points in the inner region are influenced by a gradient bias affecting the slope of the curve.

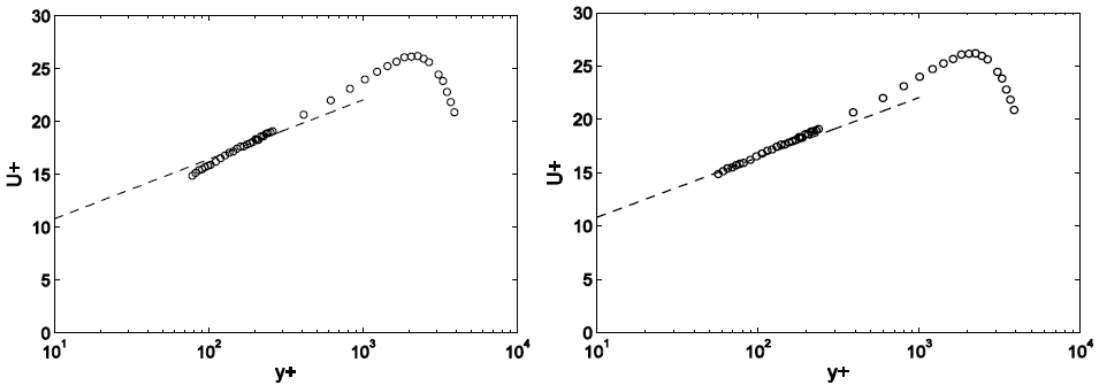

Figure A7: Streamwise mean velocity in the cold inlet pipe plotted in wall-coordinates. In the left plot, the original coordinates are used, while in the right plot the profile is shifted $\Delta y = -0.7$ mm. The dashed line is $U^+ = 1/0.41 \ln(y^+) + 5.2$.

A3.2 Branch Pipe: InHo

As mentioned earlier, the inlet velocity profiles had been measured earlier (Westin et al., 2008) when measurements were carried out with a main/branch flow ratio of 2. In the present measurements, the flowrate in the hot inlet has been kept the same, so the same velocity profiles can be applied for the present case (flow ration 1.5).

Figures A8, A9 show the axial and transverse velocity data for the hot water inlet pipe, measured at a cross-section $-3.1D_1$ upstream of the centre of the tee. Recalling that this inlet pipe is considerably shorter than the cold inlet pipe (only 20 diameters compared with 80 diameters for the cold inlet), fully developed turbulent pipe flow cannot be expected. This fact is clear already from the mean streamwise (x-direction) velocity profile shown in Fig. A8. This has a more "top hat" shape than that shown for the cold inlet in Fig. A5. The centreline velocity in the hot inlet pipe is $U_{cl} = 1.11\ U_{bulk} \approx 0.86$ m/s. Note again how the velocities have been scaled for these Figures: the mean streamwise (axial) velocity is scaled with respect to the mean bulk velocity, U_{bulk}, while all others are scaled with respect to the centreline velocity, U_{cl}.

All profiles indicate a flow with developing boundary layers on the pipe wall, while the central region of the pipe shows characteristics similar to a mainly undisturbed free stream with a turbulence level of approximately 1.5% with respect to the centreline velocity, the values signifying a generally low level of turbulence. The higher moments (skewness, S, and flatness, F) exhibit some scatter, but it is still possible to detect local peaks in both quantities close to the edge of the growing boundary layer. Flatness is a good indicator of the intermittency in the flow. In the free stream, just outside the boundary layer, one can expect that the signal would be rather undisturbed, except at instances when strong disturbances emanate from the boundary layer. The large flatness values (7–8) indicate the location of the outer edge of the boundary layer to be at $r/R \approx 0.5$.

It was preferred to perform these measurements under isothermal conditions, since the changes in the refractive index of the water due the temperature difference ΔT caused troublesome distortions of the laser beams. However, a check was made that the flow at isothermal conditions would be similar to that in which $\Delta T \approx$ 10-20°C, as used for the temperature measurements with thermocouples. Both sets of data are included in Fig. A8, and show good correspondence. Note that some profiles (along xcl) were obtained using a mirror.

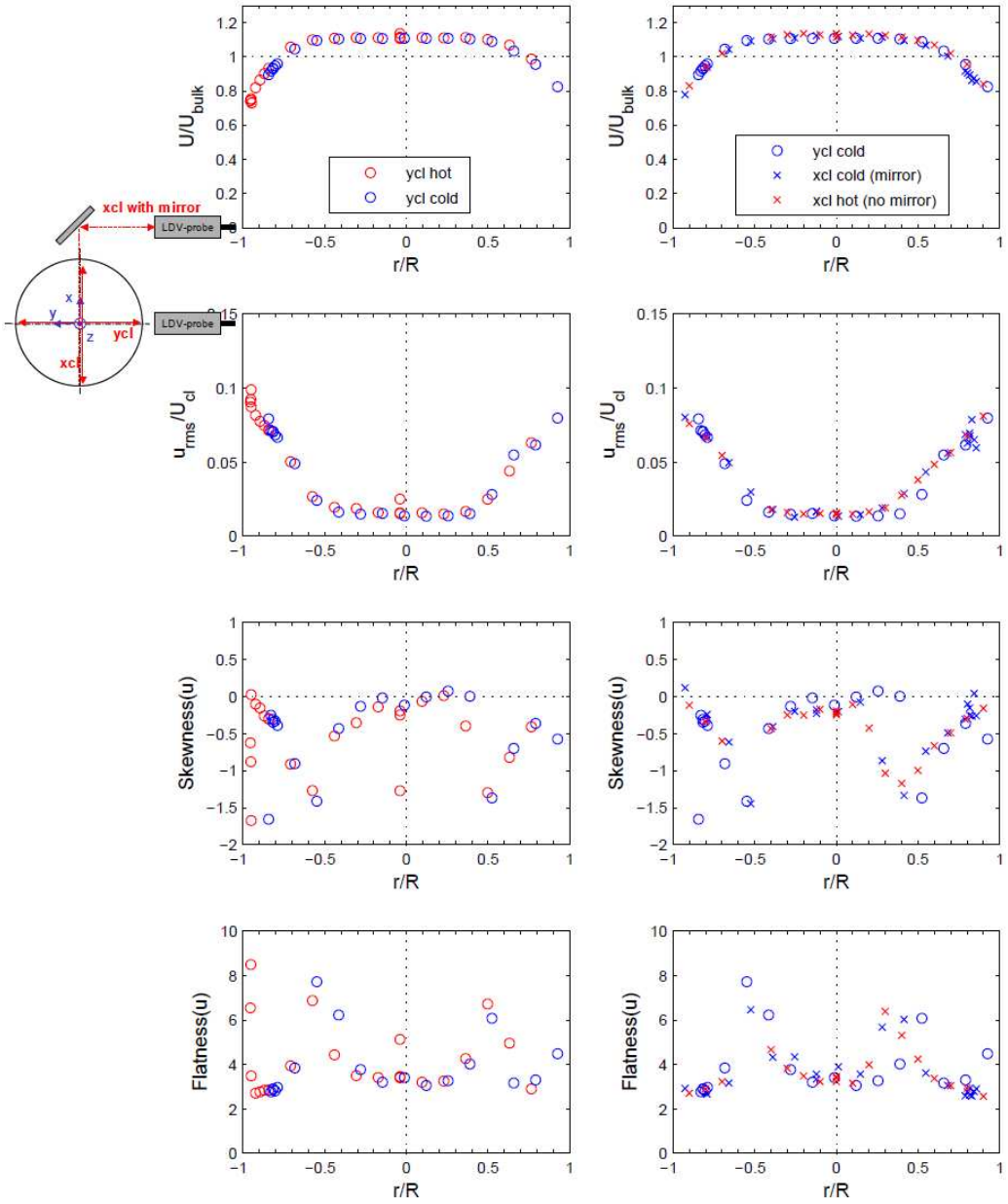

Figure A8: Streamwise (axial) velocity component for the hot inlet at z = -3.1D_1: left column, ycl with hot and cold water; right column, ycl with cold water, xcl with hot and cold water.

Figure A9 gives the measured profiles of the velocity components in the xcl and ycl directions (see inset to Fig. A8 for coordinate orientation) at the same upstream cross-section (z = -3.1D_1). Reynolds stress data are also included.

The accuracy of the electromagnetic flowmeters used for the inlet flow rates is ±0.5%. The inlet temperatures are measured using Pt100 sensors, with an accuracy of between ±0.1°C and ±0.2°C. The uncertainty in the upstream LDV measurements is estimated to be between 6% and 8% for the different measured quantities.

For convenience, all upstream LDV data are also given in tabular form at the end of the document.

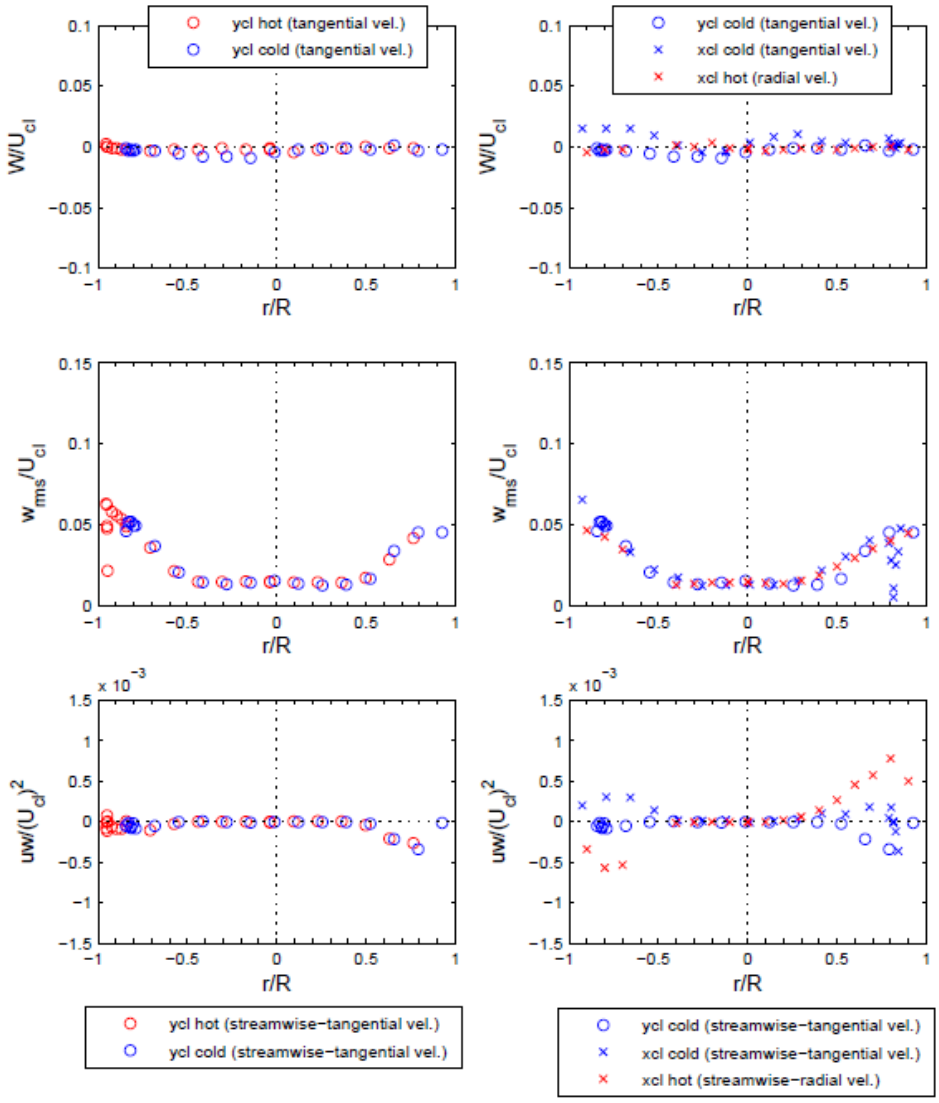

Figure A9: Scaled transverse (radial/tangential) velocity components, and Reynolds shear stresses (uw) for the hot inlet, measured at z = -3.1D_1: left column, ycl with hot and cold water; right column, ycl with cold water, and xcl with hot and cold water.

A4. DOWNSTREAM NUMERICAL DATA REQUESTED

A4.1 Introduction

Very basic quantities are requested from this benchmark, to permit flexibility in the choice of summary results, and uniform processing to obtain those results. It is assumed that most analyses will probably involve a scale-resolving turbulence modeling approach. However, the selected state information should be useful for most other approaches.

A4.2 Coordinate System Used for Reporting

The same Cartesian coordinate system developed for earlier tests in this facility will be used, as given in the previous Sections of this document, and described by Westin (2007). The origin is at the intersection of the centerlines for the main and branch pipes, with the x-axis along the main pipe's centerline, with positive direction downstream of the origin. The z-axis is along the centerline of the branch pipe, and the y axis spans the main pipe perpendicular to both main and branch centerlines. In the following discussion, use of the standard notation of u, v and w for the x, y and z components of velocity, the coordinate directions forming a right-handed set.

A4.3 Location of Instrumentation

The inside diameter of the main pipe is 140 mm (D_2). Thermocouples of 0.13mm diameter (frequency response 30 Hz) are placed approximately 1 mm (with an estimated uncertainty of about a couple of hundred microns, primarily in the positive direction) from the inner pipe wall at x = $2D_2$, $4D_2$, $6D_2$, $8D_2$, $10D_2$, $15D_2$ and $20D_2$. Taking 0° to be the top of the main pipe (y=0, z=70mm), thermocouple locations around the circumference of the pipe are given in Table A5. Angles in the Table increase in a counter-clockwise direction if the viewing perspective is from the tee junction (coordinate origin) towards the thermocouples (looking in the positive x-direction).

PIV data are available roughly spanning 1 to 5 hydraulic diameters downstream of the tee junction in the x-y and x-z planes intersecting the pipe's centerline.

Table A5. Thermocouple Locations

Location on x axis	**Angular Positions (Degrees)**
2 D_2	0, 90, 180, 270
4 D_2	0, 90, 180, 270
6 D_2	0, 90, 180, 270
8 D_2	0, 90, 180, 270
10 D_2	0, 90, 180, 270
15 D_2	0, 180
20 D_2	0, 180

A4.4 Transient Data to be Reported

Prior to the period of reported data, it is the participant's responsibility to run the simulation for a long enough time interval for time-averaged velocities to become steady. Past

simulations of this facility have accomplished this in two to four seconds, though these times should be used as a guide only. After this initial period, all transient data are to be reported at every 0.001 seconds for at least the last 5 seconds of the transient calculation, and for no more than 20 seconds. If time step sizes other than the 0.001s required for the analysis are used in the calculation, participants shall report their method for data conversion.

A non-dimensional temperature T^* shall be reported at each thermocouple location. T^* is the actual temperature minus the cold flow inlet temperature, divided by the difference between hot and cold inlet temperatures: that is,

$$T^* = \frac{T - T_{cold}}{T_{hot} - T_{cold}}$$

This is the same definition used in the paper by Frank et al. (2008). For the present benchmark case, the values T_{hot} = 36°C and T_{cold} = 19°C are to be used.

Velocities shall be reported at x = $1.6D_2$, $2.6D_2$, $3.6D_2$, and $4.6D_2$ along two lines perpendicular to the flow: horizontal (-70mm<y<70mm, z=0), and vertical (-70mm<z<70mm, y=0). To characterize the velocity field, we are asking for all three resolved components of the velocities at each reported point, and the turbulent kinetic energy (k_{SGS}) from your subgrid turbulence model (if available). Results should be reported at no less than 20 and no more than 50 points along each line segment.

In addition to the basic data, we request a characterization of your CFD methodology and mesh in an accompanying document (typically 1-2 pages). As a minimum, please provide the time step size (or range) used in the transient, range of y^+ (wall normal coordinate), total number of nodes/meshes used for the calculation, and, in each of the coordinate directions:

- an average number of cells (N_x, N_y, N_z);
- minimum cell length (Δx_{min}, Δy_{min}, Δz_{min});
- maximum cell length (Δx_{max}, Δy_{max}, Δz_{max}).

Also, summarize other mesh configurations that you used to estimate errors associated with spatial discretization, where applicable.

A4.4.1 Transient Data File Formats

All files shall be written in ASCII text format with space-delimited fields. Values of temperatures, velocity components and turbulent kinetic energies shall be written with 8 significant digits (e.g. 1.2345678 or 1.2345678E-2). Values for time or location may be written with fewer significant digits, if appropriate.

Files containing non-dimensional **temperatures** start with a line specifying thermocouple locations for corresponding values in subsequent lines. Each entry in the line is a composite providing the axial and angular location, with an integer followed by "D" followed by another integer. A portion of the first line might be:

2D0 2D90 2D180 2D270 4D0 4D45 4D90 4D135 4D180 4D225 …

Subsequent lines start with the time, and the remainder of the line contains scaled temperatures at that time, located at positions provided in the first line of the file.

Files with **velocity components** or **turbulent kinetic energy** begin with a line listing the y or z positions at which the values are located. Values are in millimetres, and in the range -70 to 70. With a very coarse sampling of results, an example of this line would be

-69.0 -60.0 -40.0 -20.0 0.0 20.0 40.0 60.0 69.0

Subsequent lines start with the time, and the remainder of the numbers in the line are CFD results interpolated to the positions provided in the first line of the file.

A4.4.2 Transient Data File Names

To enable automated processing of results, all data files must follow the same naming convention. All temperature results shall be provided in a single file named "temperatures.txt". Results for velocity components and turbulent kinetic energy are divided into files by data type, axial location, and direction of line in space (horizontal or vertical).

The specific file names and contents are:

u1.6Dh.txt	x component of velocity 1.6 diameters downstream of the tee junction for z=0 and -70mm<y<70mm (horizontal line);
u1.6Dv.txt	x component of velocity 1.6 diameters downstream of the tee junction for y=0 and -70mm<z<70mm (vertical line);
v1.6Dh.txt	y component of velocity 1.6 diameters downstream of the tee junction for z=0 and -70mm<y<70mm (horizontal line);
v1.6Dv.txt	y component of velocity 1.6 diameters downstream of the tee junction for y=0 and -70mm<z<70mm (vertical line);
w1.6Dh.txt	z component of velocity 1.6 diameters downstream of the tee junction for z=0 and -70mm<y<70mm (horizontal line);
w1.6Dv.txt	z component of velocity 1.6 diameters downstream of the tee junction for y=0 and -70mm<z<70mm (vertical line);
k1.6Dh.txt	subgrid turbulent kinetic energy 1.6 diameters downstream of the tee junction for z=0 and -70mm<y<70mm (horizontal line);
k1.6Dv.txt	subgrid turbulent kinetic energy 1.6 diameters downstream of the tee junction for y=0 and -70mm<z<70mm (vertical line).

This set of eight files is repeated three more times with the "1.6" in the title and description replaced by "2.6", "3.6", and "4.6" to capture results at these three other locations downstream of the tee junction.

A4.5 Time-Averaged Data to be Reported

In addition to transient data, we ask participants to provide:

- time-averaged values for all three velocity components;
- RMS values of the fluctuating portions of all three velocity components, as well as of the Reynolds shear stresses; and
- Time-average of the subgrid turbulent kinetic energy, if available.

This information shall be reported at x=1.6D, 2.6D, 3.6D, and 4.6D, along two lines perpendicular to the flow: horizontal (-70mm<y<70mm, z=0), and vertical (-70mm<z<70mm, y=0). As with transient data, results should be reported at no less than 20 and no more than 50 points along each line segment.

A4.5.1 Time-Averaged Data File Formats

As before, all files shall be written in ASCII text format with space-delimited fields. Time-averaged values shall be written with 8 significant digits (e.g. 1.2345678 or 1.2345678E-2). Values for times and locations may be written with fewer significant digits, if appropriate.

Files for time-averaged data start with a line listing the beginning and ending time of the window used for averaging. The next line contains y or z positions at which the values are located (same information as the first line of a corresponding transient file). Values are in millimetres, and in the range -70 to 70. The third line contains time-averaged values for the x component of velocity at the locations provided in the second line. The fourth line contains time-averaged values for the y component of velocity, and the fifth line contains time-averaged values for the z component of velocity. Lines six through eight contain RMS values of the x, y, and z components of the velocity fluctuations in the respective coordinate directions. If the information is available, a ninth line contains the time-averaged values of the subgrid turbulent kinetic energy.

A4.5.2 Time-Averaged Data File Names

To enable automated processing of results, all data files must follow the same naming convention. Files are generated by axial location and direction of line in space used to sample data (horizontal or vertical). The specific file names and contents are:

avg1.6Dh.txt	time-averaged data 1.6 diameters downstream of the tee junction for z=0 and -70mm<y<70mm (horizontal line);
avg1.6Dv.txt	time-averaged data 1.6 diameters downstream of the tee junction for y=0 and -70mm<z<70mm (vertical line);
avg2.6Dh.txt	time-averaged data 2.6 diameters downstream of the tee junction for z=0 and -70mm<y<70mm (horizontal line);
avg2.6Dv.txt	time-averaged data 2.6 diameters downstream of the tee junction for y=0 and -70mm<z<70mm (vertical line);
avg3.6Dh.txt	time-averaged data 3.6 diameters downstream of the tee junction for z=0 and -70mm<y<70mm (horizontal line);
avg3.6Dv.txt	time-averaged data 3.6 diameters downstream of the tee junction for y=0 and -70mm<z<70mm (vertical line);
avg4.6Dh.txt	time-averaged data 4.6 diameters downstream of the tee junction for z=0 and -70mm<y<70mm (horizontal line);
avg4.6Dv.txt	time-averaged data 4.6 diameters downstream of the tee junction for y=0 and -70mm<z<70mm (vertical line).

A4.6 Transmission of Results

Start by creating a text file named “Information.txt”. The first line of the file contains a comma-delimited list of the authors of the study. The second line contains the name of your organization, and the third line contains the name of the CFD program that you used. The fourth line contains an acronym, or brief phrase, describing your choice of turbulence model. For example:
B. Smith, G. Zigh
OECD/NEA
ANSYS-CFX
SAS-SST

Use GNU tar or a zip utility to create a compressed archive containing Information.txt, temperatures.txt, the 32 files for transient velocity components and turbulent kinetic energies, and the 8 files containing time-averaged information. If your modelling approach does not include a subgrid turbulence model, or the subgrid turbulent kinetic energy cannot be obtained (directly or through post-processing), then do not include the 8 files associated with transient subgrid turbulent kinetic energy. The scripts used to post-process the CFD results will automatically note and adjust for absence of these subgrid-scale data.

The file shall have a name that begins with “TeeResults”, followed by a hyphen, followed by the initials of the first-listed participant, followed by another hyphen, followed by initials for the participating organization. The suffix for the file name will be either tgz or zip. Examples are:

“TeeResults-JHM-USNRC.tgz” or “TeeResults-BS-PSI.zip”.

A5. CONCLUDING REMARKS

A5.1 Organizing Committee

Brian L. Smith, PSI, Switzerland
Kristian Angele, Vattenfall R&D, Sweden
John H. Mahaffy, US NRC, USA
Dominique Bestion, CEA, France
Ghani Zigh, US NRC, USA
Jong-Chull Jo, OECD/NEA, France (Secretariat)

A5.2 Schedule

May 20, 2009	Kick-Off Meeting
June 15, 2009 (latest)	Distribution of Draft Version of Benchmark Specifications
June 30, 2009	Deadline for comment/queries from participants concerning Benchmark Specifications
July 15, 2009 (earliest)	Distribution of Final Version of Benchmark Specifications
April 30, 2010	Deadline for Receipt of Simulation Results
June 30, 2010 (latest)	Open Benchmark Meeting (Release of Test Data)
Sept. 30, 2010 (latest)	Presentation of Results and Synthesis at CFD4NRS-3 Workshop

To ensure that there are no errors, ambiguities, etc. in the specifications, the latest date of June 15, 2009 is set for the initial distribution of the draft benchmark specifications, some 3 weeks after the kick-off meeting. Participants are requested to communicate any queries/comments within 15 days. Final specifications will then be issued, earliest July 15, 2009. The participants then have more than 9 months to perform the simulations and submit their results to the organizers.

This benchmark activity is an integral part of the CFD4NRS-3 Workshop, and the scheduling is part due to the timing of this event (in the fall of 2010). However, it is intended to release the data ahead of this time. An *Open Benchmark Meeting* will be organized in June 2010, at which time the measured data downstream of the junction will be released for the first time.

The synthesis of the blind benchmark results will be undertaken by J. H. Mahaffy, US NRC, and he will present his findings in an *Invited Lecture* at the CFD4NRS-3 Workshop, which will take place in the Washington DC area: provisional date 14-16 September 2010. The Workshop will be under joint OECD/NEA and IAEA sponsorship, as with previous workshops in the series. A paper will also be prepared to accompany the Invited Lecture, and will be part of the official conference proceedings (to be issued early in 2011).

It is hoped that many participants will take the opportunity to display their results at this Workshop, and a special Poster Session is being organized for this purpose. It will not be necessary to produce an accompanying paper in support of the poster. However, if more than the blind benchmark simulation has been performed, for example a comparison of several turbulence modelling approaches, a full paper can be submitted to the Workshop organizers in the usual way for consideration for inclusion in the technical programme. The number of such papers will be limited, however.

A5.3 Submittal Procedures

In order to be able to efficiently handle and compare calculated and measured data, all participants are requested to adhere STRICTLY to the formatting requested in Section A4. Datasets not conforming to the specified norms will be returned to the participant for correction.

The deadline for submission of code predictions is April 30, 2010. Earlier submissions will be very welcome, and will considerably ease the burden on the organizers. Later submissions will be accepted or refused at the discretion of the organizing committee. Only one submission per participant will be processed.

A special webpage will be created on an appropriate website to which participants will be able to upload their results. Details will be distributed once the webpage is functional. Individual usernames and passwords will be allocated, and all data sets will be regarded as confidential. Access to the data will only be available to the owner and to J. H. Mahaffy. After uploading, participants are advised to download their datasets and compare with the originals to ensure that perfect transmission has been accomplished. Each participant will have the opportunity to exchange the dataset submitted for a newer version, but only up to the time of the Open Benchmark Meeting, at which time no further user access to the website will be possible.

After the test data are released at the Open Benchmark Meeting (June 2010, precise date to be announced), no more submissions will be accepted. **Additionally, participants will thereafter not be permitted to withdraw their submissions.**

Participants are free to repeat their calculations once they have the test data, and display the details at the special Poster Session at the CFD4NRS-3 Workshop, as desired. However, only the "blind" code predictions will be considered for the synthesis.

REFERENCES

ASME Steam Tables, American Society of Mechanical Engineers, New York, (1967).

Frank, Th., Adlakha, M., Lifante, C., Prasser, H.-M., Menter, F. "Simulation of Turbulent and Thermal Mixing in T-Junctions Using URANS and Scale-Resolving Turbulence Models in ANSYS CFX," Proc. XCFD4NRS, Grenoble, France, Sept. 10-12, 2008.

Incropera, F. P., DeWitt, P. *Fundamentals of Heat and Mass Transfer*, 3rd ed., John Wiley & Sons, New York, 1990.

Tennekes H., Lumley, J. L. *A First Course in Turbulence*, MIT Press, 1972.

Westin, J. "Thermal Mixing in a T-Junction. Model Tests at Vattenfall Research and Development AB 2006. Boundary Conditions and List of Available Data for CFD Validation," Vattenfall Memo U 07-26 (2007).

Westin, J., et al. (2008) High-cycle thermal fatigue in mixing Tees. Large-Eddy Simulations compared to a new validation experiment, ICONE16-48731, 16th International Conference on Nuclear Engineering, Orlando, Florida, USA, May 11-15, 2008.

Zagarola, M. V., Smits, A. J. "Mean-Flow Scaling of Turbulent Pipe Flow", J. Fluid Mech., **373**, 33-79 (1998).

UPSTREAM DIGITAL DATA

Main Pipe: InCo (Figure A5)

r/R-zcl	U/Ubulk-ycl	urms/Ucl	Skew(u)	Flat(u)	W/Ucl	wrms/ucl	Skew(w)	Flat(w)
-8.14E-01	9.23E-01	7.67E-02	-3.48E-01	2.89E+00	-9.89E-03	4.35E-02	8.10E-02	2.92E+00
-6.71E-01	1.00E+00	6.87E-02	-3.09E-01	2.83E+00	-1.76E-02	4.16E-02	2.09E-01	3.27E+00
-5.29E-01	1.07E+00	6.09E-02	-3.98E-01	2.96E+00	-1.76E-02	3.78E-02	3.24E-01	3.55E+00
-3.86E-01	1.11E+00	5.33E-02	-5.01E-01	3.24E+00	-1.43E-02	3.47E-02	3.10E-01	3.40E+00
-2.43E-01	1.15E+00	4.42E-02	-5.10E-01	3.40E+00	-1.21E-02	3.10E-02	2.59E-01	3.48E+00
-1.00E-01	1.16E+00	3.91E-02	-4.98E-01	3.44E+00	-1.54E-02	2.90E-02	1.92E-01	3.74E+00
4.29E-02	1.17E+00	3.81E-02	-4.26E-01	3.38E+00	-1.43E-02	2.80E-02	-5.90E-02	3.70E+00
1.86E-01	1.16E+00	4.19E-02	-4.92E-01	3.26E+00	-1.87E-02	3.02E-02	-2.71E-01	3.64E+00
3.29E-01	1.13E+00	4.97E-02	-4.38E-01	3.21E+00	-9.89E-03	3.33E-02	-2.77E-01	3.46E+00
4.71E-01	1.08E+00	5.86E-02	-4.80E-01	3.06E+00	-1.10E-02	3.62E-02	-3.32E-01	3.44E+00
9.00E-01	8.45E-01	8.23E-02	-1.21E-01	2.64E+00	-9.89E-03	4.18E-02	-1.02E-01	3.48E+00

r/R-ycl	U/Ubulk-ycl	urms/Ucl	Skew(u)	Flat(u)	W/Ucl	wrms/ucl	Skew(w)	Flat(w)
8.19E-01	9.37E-01	7.88E-02	-1.78E-01	2.61E+00	-9.89E-03	4.88E-02	-7.00E-03	3.42E+00
7.23E-01	9.81E-01	7.49E-02	-1.44E-01	2.62E+00	-1.32E-02	4.78E-02	1.20E-02	3.25E+00
6.27E-01	1.02E+00	6.99E-02	-2.32E-01	2.83E+00	-1.21E-02	4.54E-02	-7.00E-03	3.31E+00
5.31E-01	1.07E+00	6.46E-02	-3.72E-01	2.88E+00	-1.32E-02	4.33E-02	-4.90E-02	3.25E+00
4.36E-01	1.10E+00	5.98E-02	-4.07E-01	2.99E+00	-1.32E-02	3.96E-02	-5.80E-02	3.22E+00
2.44E-01	1.15E+00	4.58E-02	-4.84E-01	3.39E+00	-1.54E-02	3.23E-02	-4.40E-02	3.65E+00
1.49E-01	1.16E+00	4.14E-02	-5.78E-01	3.63E+00	-1.43E-02	2.97E-02	-1.46E-01	3.86E+00
5.29E-02	1.18E+00	3.87E-02	-4.05E-01	3.27E+00	-1.43E-02	2.87E-02	-3.80E-02	3.72E+00
-4.29E-02	1.17E+00	3.81E-02	-4.84E-01	3.53E+00	-1.43E-02	2.87E-02	-6.00E-02	3.59E+00
-1.39E-01	1.17E+00	4.07E-02	-5.40E-01	3.52E+00	-1.54E-02	3.02E-02	6.10E-02	3.85E+00
-2.34E-01	1.15E+00	4.51E-02	-4.96E-01	3.39E+00	-1.32E-02	3.31E-02	-1.40E-02	3.61E+00
-3.30E-01	1.13E+00	4.99E-02	-4.99E-01	3.26E+00	-1.43E-02	3.58E-02	2.00E-03	3.68E+00
-4.26E-01	1.11E+00	5.58E-02	-4.38E-01	3.14E+00	-1.21E-02	3.90E-02	1.50E-02	3.49E+00
-5.21E-01	1.08E+00	6.16E-02	-3.96E-01	3.01E+00	-1.43E-02	4.12E-02	-2.90E-02	3.39E+00
-6.17E-01	1.04E+00	6.76E-02	-3.31E-01	2.80E+00	-1.43E-02	4.49E-02	-2.40E-02	3.31E+00
-7.13E-01	9.87E-01	7.15E-02	-2.67E-01	2.85E+00	-1.32E-02	4.80E-02	-3.50E-02	3.30E+00
-8.09E-01	9.27E-01	7.85E-02	-2.29E-01	2.88E+00	-1.43E-02	5.07E-02	1.60E-02	3.32E+00
-9.04E-01	8.19E-01	8.34E-02	-8.20E-02	2.76E+00	-1.21E-02	5.56E-02	-2.20E-02	3.28E+00
-8.79E-01	8.56E-01	8.11E-02	-1.17E-01	2.83E+00	-1.21E-02	5.40E-02	-3.90E-02	3.26E+00
-8.83E-01	8.51E-01	8.16E-02	-1.19E-01	2.75E+00	-1.32E-02	5.46E-02	4.00E-03	3.33E+00
-8.87E-01	8.49E-01	8.18E-02	-9.10E-02	2.73E+00	-1.21E-02	5.45E-02	1.80E-02	3.26E+00
-8.91E-01	8.46E-01	8.33E-02	-1.32E-01	2.70E+00	-1.32E-02	5.46E-02	-3.00E-03	3.26E+00
-8.95E-01	8.35E-01	8.23E-02	-9.70E-02	2.67E+00	-1.21E-02	5.51E-02	-3.10E-02	3.30E+00
-8.99E-01	8.35E-01	8.35E-02	-9.70E-02	2.74E+00	-1.21E-02	5.55E-02	9.00E-03	3.37E+00
-9.02E-01	8.21E-01	8.37E-02	-2.80E-02	2.74E+00	-1.21E-02	5.63E-02	-2.60E-02	3.43E+00
-9.06E-01	8.23E-01	8.32E-02	-6.20E-02	2.76E+00	-1.32E-02	5.64E-02	-5.30E-02	3.25E+00
-9.10E-01	8.12E-01	8.24E-02	-5.60E-02	2.75E+00	-1.21E-02	5.58E-02	8.00E-03	3.21E+00
-9.14E-01	8.05E-01	8.52E-02	-4.50E-02	2.65E+00	-1.10E-02	5.69E-02	-7.70E-02	3.27E+00
-9.18E-01	8.00E-01	8.40E-02	-9.00E-03	2.72E+00	-1.10E-02	5.70E-02	-7.80E-02	3.31E+00
-9.22E-01	7.92E-01	8.53E-02	-4.70E-02	2.78E+00	-9.89E-03	5.66E-02	-2.10E-02	3.31E+00
-9.25E-01	7.91E-01	8.22E-02	-1.10E-02	2.75E+00	-1.10E-02	5.81E-02	-2.90E-02	3.25E+00
-9.29E-01	7.82E-01	8.53E-02	-3.40E-02	2.69E+00	-9.89E-03	5.78E-02	-2.80E-02	3.35E+00
-9.33E-01	7.71E-01	8.59E-02	-4.50E-02	2.76E+00	-9.89E-03	5.76E-02	-1.50E-02	3.31E+00
-9.37E-01	7.65E-01	8.73E-02	-1.30E-02	2.74E+00	-1.10E-02	5.85E-02	2.90E-02	3.28E+00
-9.41E-01	7.54E-01	8.73E-02	-5.70E-02	2.75E+00	-9.89E-03	5.92E-02	-5.80E-02	3.25E+00
-9.44E-01	7.42E-01	8.54E-02	-3.80E-02	2.78E+00	-9.89E-03	5.91E-02	-1.40E-02	3.34E+00
-9.48E-01	7.27E-01	8.70E-02	-3.70E-02	2.77E+00	-8.79E-03	5.86E-02	-4.80E-02	3.59E+00

-9.52E-01	7.14E-01	8.63E-02	-2.00E-02	2.79E+00	-8.79E-03	6.09E-02	-3.10E-02	3.33E+00
-9.54E-01	7.10E-01	8.73E-02	-1.30E-01	2.73E+00	-1.10E-02	6.18E-02	-3.70E-02	3.24E+00
-9.56E-01	7.04E-01	8.87E-02	-1.10E-01	2.65E+00	-9.89E-03	6.19E-02	-1.60E-02	3.24E+00
-9.58E-01	6.95E-01	8.80E-02	-1.33E-01	2.78E+00	-1.10E-02	6.31E-02	-1.10E-02	3.17E+00
-9.60E-01	6.91E-01	9.13E-02	-1.62E-01	2.80E+00	-1.10E-02	6.40E-02	-4.00E-02	3.42E+00
-9.62E-01	6.79E-01	9.25E-02	-1.64E-01	2.82E+00	-9.89E-03	6.33E-02	-5.20E-02	3.31E+00
-9.64E-01	6.68E-01	9.74E-02	-4.11E-01	3.25E+00	-1.65E-02	5.18E-02	-1.14E-01	3.01E+00

Main Pipe: InCo (Figure A6)

r/R-ycl	uw/Ucl2 (ycl)	r/R-zcl	uw/Ucl2 (zcl)	r/R-curve	uw-curve
8.19E-01	-1.70E-05	-8.14E-01	-1.07E-03	########	-1.50E-03
7.23E-01	7.83E-05	-6.71E-01	-9.26E-04	-9.00E-01	-1.35E-03
6.27E-01	4.90E-05	-5.29E-01	-7.96E-04	-8.00E-01	-1.20E-03
5.31E-01	8.61E-05	-3.86E-01	-5.77E-04	-7.00E-01	-1.05E-03
4.36E-01	6.04E-06	-2.43E-01	-3.59E-04	-6.00E-01	-9.03E-04
2.44E-01	1.78E-05	-1.00E-01	-1.85E-04	-5.00E-01	-7.54E-04
1.49E-01	9.78E-05	4.29E-02	5.13E-05	-4.00E-01	-6.06E-04
5.29E-02	2.46E-05	1.86E-01	2.63E-04	-3.00E-01	-4.57E-04
-4.29E-02	5.10E-05	3.29E-01	4.57E-04	-2.00E-01	-3.09E-04
-1.39E-01	-8.09E-06	4.71E-01	7.12E-04	-1.00E-01	-1.60E-04
-2.34E-01	1.63E-05	9.00E-01	NaN	0.00E+00	-1.19E-05
-3.30E-01	3.10E-05			1.00E-01	1.37E-04
-4.26E-01	-5.55E-06			2.00E-01	2.85E-04
-5.21E-01	1.91E-05			3.00E-01	4.34E-04
-6.17E-01	-2.66E-05			4.00E-01	5.82E-04
-7.13E-01	-6.96E-05			5.00E-01	7.31E-04
-8.09E-01	-1.15E-04			6.00E-01	8.79E-04
-9.04E-01	-8.77E-05			7.00E-01	1.03E-03
-8.79E-01	-4.43E-05			8.00E-01	1.18E-03
-8.83E-01	-8.19E-05			9.00E-01	1.32E-03
-8.87E-01	-2.38E-05			1.00E+00	1.47E-03
-8.91E-01	-6.82E-05				
-8.95E-01	-1.09E-04				
-8.99E-01	-3.45E-05				
-9.02E-01	-2.37E-04				
-9.06E-01	-1.93E-04				
-9.10E-01	-9.13E-05				
-9.14E-01	-4.49E-05				
-9.18E-01	5.43E-05				
-9.22E-01	-1.45E-04				
-9.25E-01	-2.99E-05				
-9.29E-01	-2.06E-05				
-9.33E-01	-1.57E-05				
-9.37E-01	-3.63E-05				
-9.41E-01	-4.20E-05				
-9.44E-01	-1.13E-04				
-9.48E-01	-4.53E-05				
-9.52E-01	-1.08E-04				
-9.54E-01	8.82E-06				
-9.56E-01	-7.96E-05				
-9.58E-01	-1.91E-04				
-9.60E-01	-1.76E-04				
-9.62E-01	-1.65E-05				
-9.64E-01	-3.73E-04				

Main Pipe: InCo (Figure A7)

y+ (dy=0)	U+ (dy=0)	y+ (dy=-0.70)	U+ (dy=-0.7)
3.91E+03	2.09E+01	3.89E+03	2.09E+01
3.70E+03	2.19E+01	3.68E+03	2.19E+01
3.50E+03	2.28E+01	3.48E+03	2.28E+01
3.29E+03	2.38E+01	3.27E+03	2.38E+01
3.09E+03	2.45E+01	3.06E+03	2.45E+01
2.67E+03	2.56E+01	2.65E+03	2.56E+01
2.47E+03	2.59E+01	2.45E+03	2.59E+01
2.26E+03	2.62E+01	2.24E+03	2.62E+01
2.06E+03	2.61E+01	2.04E+03	2.61E+01
1.85E+03	2.61E+01	1.83E+03	2.61E+01
1.65E+03	2.57E+01	1.62E+03	2.57E+01
1.44E+03	2.53E+01	1.42E+03	2.53E+01
1.23E+03	2.47E+01	1.21E+03	2.47E+01
1.03E+03	2.40E+01	1.01E+03	2.40E+01
8.23E+02	2.31E+01	8.01E+02	2.31E+01
6.17E+02	2.20E+01	5.96E+02	2.20E+01
4.11E+02	2.07E+01	3.90E+02	2.07E+01
2.06E+02	1.83E+01	1.84E+02	1.83E+01
2.59E+02	1.91E+01	2.38E+02	1.91E+01
2.51E+02	1.90E+01	2.29E+02	1.90E+01
2.43E+02	1.89E+01	2.21E+02	1.89E+01
2.35E+02	1.89E+01	2.13E+02	1.89E+01
2.26E+02	1.86E+01	2.05E+02	1.86E+01
2.18E+02	1.86E+01	1.97E+02	1.86E+01
2.10E+02	1.83E+01	1.88E+02	1.83E+01
2.02E+02	1.83E+01	1.80E+02	1.83E+01
1.93E+02	1.81E+01	1.72E+02	1.81E+01
1.85E+02	1.79E+01	1.64E+02	1.79E+01
1.77E+02	1.78E+01	1.55E+02	1.78E+01
1.69E+02	1.77E+01	1.47E+02	1.77E+01
1.60E+02	1.76E+01	1.39E+02	1.76E+01
1.52E+02	1.74E+01	1.31E+02	1.74E+01
1.44E+02	1.72E+01	1.23E+02	1.72E+01
1.36E+02	1.71E+01	1.14E+02	1.71E+01
1.28E+02	1.68E+01	1.06E+02	1.68E+01
1.19E+02	1.65E+01	9.78E+01	1.65E+01
1.11E+02	1.62E+01	8.96E+01	1.62E+01
1.03E+02	1.59E+01	8.14E+01	1.59E+01
9.87E+01	1.58E+01	7.72E+01	1.58E+01
9.46E+01	1.57E+01	7.31E+01	1.57E+01
9.05E+01	1.55E+01	6.90E+01	1.55E+01
8.64E+01	1.54E+01	6.49E+01	1.54E+01
8.23E+01	1.51E+01	6.08E+01	1.51E+01
7.82E+01	1.49E+01	5.67E+01	1.49E+01

Branch Pipe: InHo (Figure A8)

Ycl-hot

r/R	U/Ubulk	urms/Ucl	skew(u)	flat(u)
-3.87E-02	1.14E+00	1.53E-02	-2.48E-01	3.45E+00
-3.87E-02	1.11E+00	1.57E-02	-1.92E-01	3.40E+00
7.65E-01	9.87E-01	6.30E-02	-4.07E-01	2.89E+00
6.31E-01	1.07E+00	4.40E-02	-8.21E-01	4.95E+00
4.97E-01	1.10E+00	2.50E-02	-1.30E+00	6.72E+00
3.63E-01	1.11E+00	1.66E-02	-3.97E-01	4.26E+00
2.29E-01	1.11E+00	1.50E-02	1.30E-02	3.25E+00
9.53E-02	1.11E+00	1.57E-02	-6.40E-02	3.20E+00
-3.87E-02	1.11E+00	2.51E-02	-1.27E+00	5.12E+00
-1.73E-01	1.11E+00	1.60E-02	-1.40E-01	3.41E+00
-3.07E-01	1.11E+00	1.86E-02	-3.51E-01	3.50E+00
-4.41E-01	1.11E+00	1.95E-02	-5.32E-01	4.43E+00
-5.75E-01	1.10E+00	2.67E-02	-1.27E+00	6.87E+00
-7.09E-01	1.06E+00	5.03E-02	-9.12E-01	3.94E+00
-8.43E-01	9.33E-01	7.13E-02	-2.96E-01	2.85E+00
-8.43E-01	9.33E-01	7.21E-02	-3.02E-01	2.84E+00
-8.70E-01	9.01E-01	7.48E-02	-2.61E-01	2.84E+00
-8.96E-01	8.64E-01	7.76E-02	-1.54E-01	2.76E+00
-9.23E-01	8.19E-01	8.16E-02	-1.01E-01	2.71E+00
-9.50E-01	7.54E-01	8.73E-02	2.60E-02	3.48E+00
-9.47E-01	7.29E-01	1.51E-01	-2.81E+00	1.33E+01
-9.50E-01	7.51E-01	9.90E-02	-1.67E+00	1.34E+01
-9.53E-01	7.51E-01	9.24E-02	-8.79E-01	8.49E+00
-9.55E-01	7.41E-01	9.05E-02	-6.24E-01	6.55E+00

Ycl-cold

r/R	U/Ubulk	urms/Ucl	skew(u)	flat(u)
9.26E-01	8.24E-01	7.98E-02	-5.74E-01	4.48E+00
7.92E-01	9.55E-01	6.16E-02	-3.61E-01	3.31E+00
6.58E-01	1.03E+00	5.48E-02	-6.99E-01	3.17E+00
5.24E-01	1.09E+00	2.82E-02	-1.37E+00	6.08E+00
3.90E-01	1.10E+00	1.51E-02	5.00E-03	4.02E+00
2.56E-01	1.11E+00	1.36E-02	7.50E-02	3.27E+00
1.22E-01	1.11E+00	1.34E-02	-4.00E-03	3.05E+00
-1.24E-02	1.11E+00	1.36E-02	-1.15E-01	3.41E+00
-1.46E-01	1.11E+00	1.54E-02	-1.80E-02	3.20E+00
-2.80E-01	1.11E+00	1.49E-02	-1.31E-01	3.77E+00
-4.14E-01	1.10E+00	1.62E-02	-4.32E-01	6.22E+00
-5.48E-01	1.09E+00	2.42E-02	-1.41E+00	7.72E+00
-6.82E-01	1.04E+00	4.90E-02	-9.06E-01	3.85E+00
-8.16E-01	9.29E-01	7.08E-02	-3.08E-01	2.91E+00
-7.90E-01	9.59E-01	6.67E-02	-3.89E-01	2.96E+00
-8.03E-01	9.46E-01	6.83E-02	-3.30E-01	2.81E+00
-8.16E-01	9.33E-01	7.04E-02	-3.45E-01	2.88E+00
-8.30E-01	9.17E-01	7.13E-02	-2.52E-01	2.77E+00
-8.43E-01	8.95E-01	7.92E-02	-1.66E+00	1.71E+01

Xcl-hot

r/R	U/Ubulk	urms/Ucl	skew(u)	flat(u)
0.00E+00	1.14E+00	1.53E-02	-2.48E-01	3.45E+00
9.00E-01	8.41E-01	8.10E-02	-1.59E-01	2.56E+00
8.00E-01	9.56E-01	6.76E-02	-2.95E-01	2.93E+00
7.00E-01	1.02E+00	5.64E-02	-4.88E-01	3.04E+00
6.00E-01	1.07E+00	4.84E-02	-6.63E-01	3.37E+00
5.00E-01	1.10E+00	3.80E-02	-9.95E-01	4.24E+00
4.00E-01	1.12E+00	2.76E-02	########	5.31E+00
3.00E-01	1.13E+00	1.92E-02	########	6.39E+00
2.00E-01	1.13E+00	1.64E-02	-4.25E-01	3.99E+00
1.00E-01	1.13E+00	1.50E-02	-1.05E-01	3.16E+00
0.00E+00	1.13E+00	1.47E-02	-2.21E-01	3.23E+00
-1.00E-01	1.13E+00	1.54E-02	-1.72E-01	3.22E+00
-2.00E-01	1.14E+00	1.50E-02	-2.50E-01	3.48E+00
-3.00E-01	1.13E+00	1.60E-02	-2.48E-01	3.82E+00
-4.00E-01	1.12E+00	1.79E-02	-4.30E-01	4.66E+00
-7.00E-01	1.02E+00	5.46E-02	-6.00E-01	3.23E+00
-8.00E-01	9.40E-01	6.68E-02	-3.38E-01	2.90E+00
-9.00E-01	8.31E-01	7.60E-02	-1.16E-01	2.71E+00
0.00E+00	1.11E+00	1.57E-02	-1.92E-01	3.40E+00

Xcl-cold

r/R	U/Ubulk	urms/Ucl	skew(u)	flat(u)
-9.26E-01	7.78E-01	8.03E-02	1.19E-01	2.92E+00
-7.92E-01	9.38E-01	6.72E-02	-2.38E-01	2.67E+00
-6.58E-01	1.04E+00	4.96E-02	-6.15E-01	3.16E+00
-5.24E-01	1.09E+00	2.98E-02	########	6.46E+00
-3.90E-01	1.11E+00	1.82E-02	-4.04E-01	4.32E+00
-2.56E-01	1.11E+00	1.28E-02	-1.98E-01	4.34E+00
-1.22E-01	1.12E+00	1.63E-02	-2.25E-01	3.56E+00
-1.22E-01	1.12E+00	1.68E-02	-1.78E-01	3.34E+00
1.24E-02	1.12E+00	1.35E-02	-2.04E-01	3.89E+00
1.46E-01	1.11E+00	1.46E-02	-7.60E-02	3.56E+00
2.80E-01	1.11E+00	1.91E-02	-8.65E-01	5.68E+00
4.14E-01	1.10E+00	2.88E-02	########	6.02E+00
5.48E-01	1.07E+00	4.34E-02	-7.38E-01	3.61E+00
6.82E-01	1.00E+00	5.61E-02	-4.90E-01	3.05E+00
8.16E-01	8.94E-01	6.96E-02	-2.55E-01	2.94E+00
7.90E-01	9.15E-01	6.87E-02	-3.05E-01	2.59E+00
8.03E-01	9.05E-01	6.28E-02	-1.02E-01	2.77E+00
8.16E-01	8.92E-01	6.76E-02	-1.52E-01	2.62E+00
8.30E-01	8.62E-01	7.86E-02	-2.64E-01	2.58E+00
8.43E-01	8.76E-01	6.52E-02	4.30E-02	2.78E+00
8.57E-01	8.55E-01	5.97E-02	-2.57E-01	2.90E+00

Branch Pipe: InHo (Figure A9)

Ycl-hot

r/R	W/Ucl	wrms/Ucl	uw/Ucl^2
-3.87E-02	-2.31E-03	1.49E-02	-1.04E-05
-3.87E-02	-1.16E-03	1.45E-02	-1.87E-06
7.65E-01	-1.16E-03	4.17E-02	-2.66E-04
6.31E-01	-1.16E-03	2.86E-02	-2.11E-04
4.97E-01	0.00E+00	1.71E-02	-4.41E-05
3.63E-01	-1.16E-03	1.42E-02	2.41E-06
2.29E-01	-2.31E-03	1.45E-02	7.22E-06
9.53E-02	-4.62E-03	1.43E-02	1.20E-06
-3.87E-02	-2.31E-03	1.46E-02	5.35E-07
-1.73E-01	-2.31E-03	1.50E-02	-1.07E-06
-3.07E-01	-1.16E-03	1.47E-02	-2.54E-06
-4.41E-01	-2.31E-03	1.48E-02	1.07E-06
-5.75E-01	-2.31E-03	2.13E-02	-2.97E-05
-7.09E-01	-3.47E-03	3.58E-02	-1.06E-04
-8.43E-01	-2.31E-03	5.08E-02	-4.41E-05
-8.43E-01	-2.31E-03	4.89E-02	4.28E-06
-8.70E-01	-2.31E-03	5.35E-02	-9.05E-05
-8.96E-01	-1.16E-03	5.57E-02	-9.13E-05
-9.23E-01	-1.16E-03	5.79E-02	-6.27E-05
-9.50E-01	0.00E+00	4.75E-02	-1.16E-04
-9.47E-01	0.00E+00	2.15E-02	1.74E-06
-9.50E-01	0.00E+00	4.92E-02	7.60E-05
-9.53E-01	0.00E+00	6.23E-02	-8.95E-06
-9.55E-01	2.31E-03	6.29E-02	-8.21E-05

Ycl-cold

r/R	W/Ucl	wrms/Ucl	uw/Ucl^2
9.26E-01	-2.31E-03	4.52E-02	-1.54E-05
7.92E-01	-3.47E-03	4.52E-02	-3.41E-04
6.58E-01	1.16E-03	3.39E-02	-2.16E-04
5.24E-01	-2.31E-03	1.65E-02	-2.76E-05
3.90E-01	-1.16E-03	1.29E-02	-6.50E-06
2.56E-01	-1.16E-03	1.25E-02	-7.23E-06
1.22E-01	-2.31E-03	1.35E-02	-6.63E-06
-1.24E-02	-4.62E-03	1.54E-02	-4.64E-06
-1.46E-01	-9.25E-03	1.41E-02	-1.33E-05
-2.80E-01	-8.09E-03	1.32E-02	-6.74E-06
-4.14E-01	-8.09E-03	1.45E-02	5.04E-06
-5.48E-01	-5.78E-03	2.06E-02	-4.20E-06
-6.82E-01	-3.47E-03	3.68E-02	-5.27E-05
-8.16E-01	-2.31E-03	5.19E-02	-8.20E-05
-7.90E-01	-2.31E-03	4.94E-02	-8.55E-05
-8.03E-01	-3.47E-03	4.95E-02	-2.17E-05
-8.16E-01	-2.31E-03	5.14E-02	-5.90E-05
-8.30E-01	-3.47E-03	5.17E-02	-1.75E-05
-8.43E-01	-1.16E-03	4.60E-02	-5.26E-05

Xcl-hot

r/R	W/Ucl	wrms/Ucl	uw/Ucl^2
0.00E+00	1.49E-02	1.49E-02	-1.04E-05
9.00E-01	4.47E-02	4.47E-02	5.01E-04
8.00E-01	4.00E-02	4.00E-02	7.79E-04
7.00E-01	3.51E-02	3.51E-02	5.73E-04
6.00E-01	2.94E-02	2.94E-02	4.56E-04
5.00E-01	2.40E-02	2.40E-02	2.65E-04
4.00E-01	1.87E-02	1.87E-02	1.42E-04
3.00E-01	1.55E-02	1.55E-02	5.97E-05
2.00E-01	1.35E-02	1.35E-02	1.86E-05
1.00E-01	1.39E-02	1.39E-02	-4.68E-06
0.00E+00	1.46E-02	1.46E-02	1.34E-07
-1.00E-01	1.43E-02	1.43E-02	-6.42E-06
-2.00E-01	1.43E-02	1.43E-02	-1.20E-06
-3.00E-01	1.35E-02	1.35E-02	-6.68E-06
-4.00E-01	1.28E-02	1.28E-02	-1.78E-05
-7.00E-01	3.47E-02	3.47E-02	-5.35E-04
-8.00E-01	4.24E-02	4.24E-02	-5.71E-04
-9.00E-01	4.66E-02	4.66E-02	-3.40E-04
0.00E+00	1.45E-02	1.45E-02	-1.87E-06

Xcl-cold

r/R	W/Ucl	wrms/Ucl	uw/Ucl^2
-9.26E-01	1.50E-02	6.53E-02	2.00E-04
-7.92E-01	1.50E-02	4.91E-02	3.04E-04
-6.58E-01	1.50E-02	3.31E-02	2.98E-04
-5.24E-01	9.25E-03	2.23E-02	1.39E-04
-3.90E-01	1.16E-03	1.75E-02	1.52E-05
-2.56E-01	-4.62E-03	1.23E-02	8.43E-06
-1.22E-01	-3.47E-03	1.29E-02	2.31E-05
-1.22E-01	-4.62E-03	1.27E-02	1.74E-05
1.24E-02	3.47E-03	1.28E-02	-1.11E-05
1.46E-01	8.09E-03	1.28E-02	7.46E-06
2.80E-01	1.04E-02	1.54E-02	3.24E-05
4.14E-01	4.62E-03	2.17E-02	9.86E-05
5.48E-01	3.47E-03	3.03E-02	9.27E-05
6.82E-01	-1.16E-03	4.03E-02	1.82E-04
8.16E-01	0.00E+00	5.20E-03	1.32E-06
7.90E-01	6.94E-03	3.86E-02	4.49E-05
8.03E-01	2.31E-03	2.80E-02	1.75E-04
8.16E-01	1.16E-03	1.06E-02	-1.68E-05
8.30E-01	-1.16E-03	2.52E-02	-1.22E-04
8.43E-01	2.31E-03	3.34E-02	-3.66E-04